Carbonic Anhydrase Catalysis: A Volume Profile Analysis

ARTICLE *in* THE JOURNAL OF PHYSICAL CHEMISTRY · MAY 1996

Impact Factor: 2.78 · DOI: 10.1021/jp9524791

Carbonic Anhydrase Catalysis: A Volume Profile Analysis

Xiaoping Zhang,[‡,§] Colin D. Hubbard,[†,‡] and Rudi van Eldik*[,‡]

Institute for Inorganic Chemistry, University of Erlangen-Nürnberg, Egerlandstrasse 1, 91058 Erlangen, Germany, and Department of Chemistry, University of New Hampshire, Durham, New Hampshire 03824-3598

Received: August 24, 1995; In Final Form: January 2, 1996[⊗]

The human carbonic anhydrase II catalyzed hydration of CO_2 and dehydration of HCO_3^- at low and high buffer concentrations and at low and high substrate concentrations were studied using a pH-indicator method at pressures up to 130 MPa. Activation volumes, $\Delta V^{\ddagger}$, for k^h_{cat}, k^h_{cat}/K^h_m, k^d_{cat}, and k^d_{cat}/K^d_m are 0, -9 ± 1, $+9 \pm 1$ ($+10 \pm 3$ in D_2O), and $+14.0 \pm 1.2$ cm^3 mol^{-1} in H_2O solution, respectively; they were derived from rate constants obtained in the buffer concentration independent region. The value of $\Delta V^{\ddagger}$ for both intra- and intermolecular proton-transfer steps is zero. The solvent kinetic isotope effect on k^d_{cat} is 3.6 ± 0.4 (H_2O/D_2O) at pressures up to 100 MPa. Analysis of these results indicates that nucleophilic attack of the Zn^{2+} bound hydroxyl moiety on CO_2 is associative, and that the CO_2 release and the substitution of H_2O by HCO_3^- on the zinc center are dissociative in character. The CO_2 release and a proton transfer are concerted steps during the dehydration reaction. A reaction volume profile for the catalyzed hydration of CO_2 and dehydration of HCO_3^- is constructed. When this has been analyzed in concert with that found for the uncatalyzed reactions and the kinetic results for the model complex catalyzed reactions, further mechanistic distinctions within the overall hydration/dehydration pathways of carbonic anhydrase catalysis were inferred. The nucleophilic attack of the Zn^{2+}-bound hydroxyl moiety on CO_2 takes place via an outer-sphere mechanism in which the oxygen from coordinated OH^- directly attacks the carbon of CO_2. The bicarbonate coordination with Zn^{2+} is most likely to be unidentate, and the proton of the bicarbonate species bridges two oxygen atoms, one of which coordinates with Zn^{2+} and the other binds to the carbon atom of the bicarbonate ion. Breakage and formation of the Zn−O bond are involved in the substitution reaction during which HCO_3^- is displaced by H_2O in the hydration reaction, and H_2O is displaced by HCO_3^- in the dehydration reaction.

Introduction

A key experimental variable we have frequently found to be extremely valuable in mechanistic studies is pressure. Use of it permits determination of activation volumes which combined with partial molar volumes and/or reaction volume data can be used to construct a reaction volume profile that represents the chemical process in terms of volume changes along the reaction coordinate.[1] Volume profiles have assisted in the elucidation of inorganic/organometallic reaction mechanisms and more recently also those of bioinorganic systems.[2−4] There are several reports in the literature of activation volumes for enzyme-catalyzed reactions,[5a] and a reaction volume profile has been generated for conversion of fumarate to *l*-malate catalyzed by fumarase.[5b] However, there is no report in the literature of a complete reaction profile for an enzyme-catalyzed reaction derived from employing a rapid reaction method to study both the forward and reverse reaction. In addition, the reaction volume profile for the uncatalyzed reaction is available for the present system. This paper describes the establishment of the reaction volume profile for human carbonic anhydrase II (HCA II).

Human carbonic anhydrase catalyzes the reversible hydration of CO_2 to yield bicarbonate ion and a proton with extreme efficiency (eq 1).[6−12] Our objective was to probe mechanistic

$$CO_2 + H_2O \overset{\text{HCA II}}{\rightleftharpoons} HCO_3^- + H^+ \qquad (1)$$

features of HCA II catalysis, which are as yet not completely understood, by application of the pressure variable. The specific features which will be addressed are indicated following an assessment of the current understanding of the catalysis mechanism.

There is a wealth of literature assembled by a multitude of investigators regarding reaction 1. Various methods of experimental study of the reaction in solution have been employed. These include kinetic solvent isotope (hydrogen) effects,[13] exchange of oxygen-18 between bicarbonate and water catalyzed by HCA II,[14] a carbon-13 NMR study of CO_2/HCO_3^- exchange (HCA II catalyzed),[15] catalytic measurements on HCA II in which Zn^{2+} has been substituted by other metal ions,[16] and inhibition studies of both the native enzyme and variants in which key amino acids have been substituted.[17] Computer simulation of the catalytic mechanism and subsequent theoretical calculations by a wide variety of methods have all been influential in leading toward the current understanding of the catalytic mechanism.[18−31] X-ray data[32−35] show that the Zn^{2+} ion sits at the bottom of a conical cavity where it is coordinated by the N atoms of His-94, His-96 and His-119 and by a water molecule/hydroxide ion (water-263) in a slightly distorted tetrahedral geometry. One part of the cavity is dominated by hydrophobic amino acid side chains, whereas another part has mostly a hydrophilic character. The hydrophobic part of the cavity hosts the substrate CO_2.[36,37] More than one CO_2 molecule can be within the active site region, one bound to Zn^{2+} and other additional molecules are adjacent in the hydrophobic part of the cavity.[38,39] Two water molecules have been proposed to

* Address correspondence to this author at the University of Erlangen-Nürnberg.
† University of New Hampshire.
‡ University of Erlangen-Nürnberg.
§ On leave from the Institute of Molecular Science, Shanxi University, Taiyuan, Shanxi, 030006, P. R. China.
⊗ Abstract published in *Advance ACS Abstracts,* April 15, 1996.

S0022-3654(95)02479-8 CCC: $12.00

SCHEME 1[17,29,32,40]

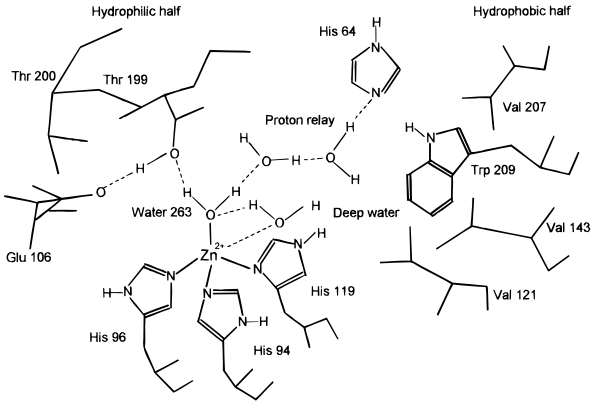

SCHEME 2

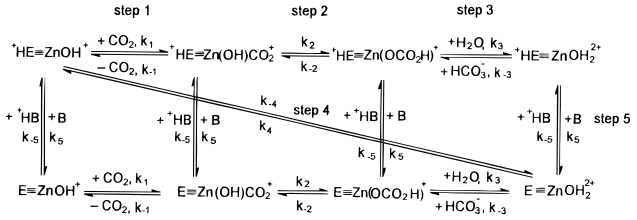

participate in the turnover reaction.[40] A simplified structure of the active center is shown in Scheme 1.

As can best be distilled from most studies a commonly accepted description of the catalytic process is the zinc hydroxide mechanism shown in Scheme 2. For the hydration of CO_2: (1) A substrate CO_2 molecule, presumably at the carbon atom, is subjected to a nucleophilic attack by the Zn^{2+} bound hydroxide moiety. (2) This results in the production of a Zn^{2+} bound bicarbonate species. (3) Then there is substitution at Zn^{2+} by water and thereby release of the product bicarbonate ion. (4) A proton from the coordinated water is transferred through a two-water-molecule bridge to a neighboring group, His-64 (intramolecular). Thus the active center is now restored to that prior to that in step 1, although since the proton is still attached to the protein backbone, the enzyme can still be formally written as $^{+}HE{\equiv}ZnOH^{+}$. The overall cycle is complete (step 5) when the proton of His-64 is transferred to the surrounding buffer medium. At low buffer concentration the rate of turnover is controlled by k_5, and at high buffer concentration k_4 controls the overall hydration.[31] The ratio k^h_{cat}/K^h_m is controlled[21] by the metal-bound water molecule. Both this ratio and k^h_{cat} have pH profiles which are typical of titration of a single group, with a pK_a close to 7, and maximal catalytic activity at high pH.[31] Ghannam et al.[41] have determined the activation enthalpy and entropy of k_{cat} and k_{cat}/K_m for the carbonic anhydrase catalyzed hydration of CO_2. Using the computer model of Rowlett,[42] the kinetic parameters for k^h_{cat} and k^h_{cat}/K^h_m were correlated with the individual steps.[41] The activation enthalpy and entropy for k^h_{cat} were attributed to the effect of temperature on the intramolecular proton-transfer step,[41] and for k^h_{cat}/K^h_m were essentially attributable to the first step given by $k_1[CO_2]$.[41]

For the reverse reaction (dehydration of HCO_3^-): (1) First there is replacement of water coordinated to Zn^{2+} by HCO_3^-. (2) Step 2 may be regarded as the generation of an active bicarbonate species $E{\equiv}Zn(OH)CO_2^+$. (3) There is subsequent release of the product CO_2, yielding $E{\equiv}ZnOH^+$. (4) Intermolecular proton transfer (buffer to enzyme, but not yet at the Zn^{2+} center) occurs. (5) Intramolecular proton transfer from the protein to the Zn^{2+} center takes place, thus regenerating the initial species for the dehydration reaction. Within the overall dehydration reaction, intermolecular proton transfer, rate constant k_{-5}, is the rate determining step at low buffer concentration.[8] At high buffer concentrations, the solvent isotope effect[13] was interpreted to indicate that intramolecular proton transfer is the rate-determining step. Both k^d_{cat} and k^d_{cat}/K^d_m have pH profiles which are typical of titration of a single group, with a pK_a close to 7, and maximal catalytic activity at low pH.[15]

There is general consistency of experimental kinetic results[41−43] with the overall mechanism of the enzyme. However, individual steps in the mechanism have not been characterized completely. Whether the first step of nucleophilic attack during the CO_2 hydration reaction proceeds through an inner-sphere or outer-sphere mechanism[44] has not been unequivocally established. The outer-sphere mechanism proposes that the oxygen from coordinated OH^- directly attacks the carbon of CO_2, while for the inner-sphere mechanism it is suggested that the oxygen from CO_2 coordinates with Zn^{2+}. Whether the binding mode of bicarbonate is bidentate or unidentate in the intermediate is still controversial.[45] How the substitution of coordinated HCO_3^- by a water molecule, or the converse, takes place in the enzyme catalyzed reaction on the basis of experimental results has not been reported. Although the release of CO_2 has been identified as dissociative in character in model complex reactions,[46] the mechanistic character of this step has yet to be established for the enzyme-catalyzed reaction.

It has in general been proposed that hydrogen bonds are formed and destroyed with nearly zero changes in volume ($\Delta\bar{V}$) for biological systems,[47] i.e., they are pressure-insensitive. The determination of the activation volumes for the intra- and intermolecular proton-transfer steps can confirm the notion that the proton-transfer steps for the HCA II catalyzed reaction occur via a hydrogen bond formed proton relay. Therefore, our objective was to obtain activation volumes for these reaction steps using high-pressure rapid reaction kinetic techniques with the aim of constructing a volume profile for the overall catalytic cycle of HCA II. From such information, mechanistic insight into the individual steps within the overall catalytic cycle, can be obtained. A better understanding of the spontaneous hydration and dehydration reactions,[48] as well as of reactions on complexes, $M(NH_3)_5OH^{2+}$ for carboxylation and $M(NH_3)_5OCO_2H^{2+}$ for decarboxylation,[46] have already been acquired using this approach.

Experimental Section

Materials. Dialyzed, lyophilized human carbonic anhydrase II (HCA II) was purchased from Sigma (3500 W-A units/mg of solid) and used directly without further purification. Stock solutions were prepared by dissolving the protein in distilled, deionized and degassed water. Enzyme concentrations were estimated from absorbance measurements at 280 nm by using a molar absorptivity of 5.6×10^4 M^{-1} cm^{-1}.[49] All reagents used were analytical reagent grade quality. The indicators and biological buffers used (without further purification) were *m*-cresol purple (Sigma), bromocresol purple (Merck), Taps (*N*-tris[hydroxymethyl]methyl-3-aminopropanesulfonic acid, Merck), and Mes (2-[*N*-morpholino]ethanesulfonic acid, Merck). Carbon dioxide (purity grade 99.995%) was purchased from Messer Griesheim. Sodium bicarbonate (A.C.S grade) was purchased from Fluka. Heavy water, D_2O (99.9 atom % D), was purchased from Aldrich.

Solution Preparation. All solutions were prepared using distilled and deionized water which had been boiled for more than 1 h immediately prior to use to remove the dissolved CO_2. A saturated solution of CO_2 was prepared by bubbling CO_2 gas into water in a vessel maintained at 25.0 °C, and dilute solutions

were made in the absence of air by coupling two syringes as described by Kahlifah.[50] Carbon dioxide concentrations were calculated on the basis of 33.8 mM at 25 °C for a saturated solution in water.[51] The method was checked by back titration with standardized barium hydroxide solution and hydrochloric acid using an automatic titrator (702 SM Titrino). Saturation was ensured by bubbling CO_2 through water for at least a half-hour before the start of each experiment, and the flow of CO_2 was maintained as long as the solution was in use. Stock solutions of sodium bicarbonate were made up by weighing an appropriate quantity and dissolving in CO_2-free water containing sodium sulfate to give the desired $NaHCO_3$ concentration and ionic strength.

Methods and Instrumentation. All atmospheric pressure kinetics were carried out on a Durrum D110 stopped-flow spectrophotometer with a glass/Kel F flow path and a 2 cm observation cuvette. Temperature was maintained at 25.0 ± 0.1 °C by thermostatted circulating fluid. A Metrohm 632 pH meter equipped with an Ingold V402-S7/120 electrode was used to determine the pH of the reaction mixture directly. All measurements at elevated pressures (up to 130 MPa) were carried out at 25.0 ± 0.1 °C in a home-built stopped-flow unit.[52] In this instrument the flow path is entirely of Kel-F, so all solutions employed in kinetic measurements do not contact metallic surfaces. Kinetic measurements with both instruments were monitored with an attached on-line data acquisition and handling system. The data were treated using the OLIS KINFIT (Bogart, Georgia) set of programs.

The reactions were followed spectrophotometrically making use of the "changing pH indicator" method as described by Khalifah.[50] The pairs of buffers and indicators, their pK_a values, wavelength of measurement, and molar absorptivities, measured under the same conditions are as follows: Mes (pK_a = 6.1), with bromocresol purple (pK_a = 6.80, λ = 420 nm, $\epsilon = 9.47 \times 10^3$ M^{-1} cm^{-1}); Taps (pK_a = 8.4) with *m*-cresol purple (pK_a = 8.3, λ = 436 nm, $\epsilon = 1.41 \times 10^4$ M^{-1} cm^{-1}).

Typical kinetic procedures are as follows: for the hydration reaction one syringe of the stopped-flow instrument contained CO_2 and the other contained HCA II, Taps buffer, *m*-cresol purple, EDTA, and Na_2SO_4. The dehydration kinetics were carried out with one syringe containing $NaHCO_3$, and the other containing HCA II, Mes buffer, bromocresol purple, EDTA, and Na_2SO_4, with the same concentrations of the latter two materials as in the hydration experiments. All solutions contained 10 μM EDTA to scavenge any extraneous heavy-metal ions.[53]

Data Treatment. Estimates of k_{cat} and k_{cat}/K_m from initial rate versus substrate concentration data were acquired using a weighted linear least-squares method with V^4 weights[54] for the double reciprocal form of the Michaelis−Menten equation. The initial rate of the hydration and dehydration reactions was determined according to[55,56]

$$\left(\frac{dx}{dt}\right)_{t=0} = -Q_0\left(\frac{dA}{dt}\right)_{t=0} = -Q_0(A_0 - A_e)\left[\frac{d\ln(A - A_e)}{dt}\right]_{t=0} = \lim_{t=0}[k_{apparent}Q_0(A - A_e)] \quad (2)$$

where $(dx/dt)_{t=0}$ represents the initial rate, (dA/dt) is the rate of change of absorbance of the indicator, and A_0 and A_e are the initial and final absorbance changes, respectively. The value of $k_{apparent}$ is obtained by fitting the absorbance-time traces with a single exponential function. Q_0 is the buffer factor which relates changes in absorbance of the indicator to changes in concentration of H^+ ion. Q_0 was measured by the method described by Kahlifah.[50] At each substrate (CO_2 or HCO_3^-) concentration, the full reaction trace is accurately recorded; this provides the value of the total absorbance change occurring in each case. The amount of CO_2 converted to HCO_3^- during the hydration reaction represents the increment of acid which generates the recorded absorbance change and conversely the amount of HCO_3^- converted to CO_2 during the dehydration reaction represents the increment of base which produces the recorded absorbance change. Equation 3 can be used in the

$$[CO_2]_0 = [HCO_3^-]_f + \frac{K_{HB}([HB^+]_0 + [HCO_3^-]_f)[HCO_3^-]_f}{K_1([B]_0 - [HCO_3^-]_f)} \quad (3)$$

calculation of the buffer factor for hydration, where the subscript f indicates the equilibrium condition pertaining after the completion of the hydration reaction, B and HB^+ refer, respectively, to the basic and protonated buffer species, subscript 0 refers to the condition at the beginning of the hydration reaction, and K_{HB} and K_1 are the buffer ionization constant and the first ionization constant of CO_2, with respective values of 8.28 and 6.0 at 25 °C and 0.1 M ionic strength. The initial concentration of CO_2 is equal to the sum of the equilibrium concentrations of CO_2 and HCO_3^-. $[HB^+]_0$ and $[B]_0$ are calculated from our experimentally determined values of pK_{HB} and the initial pH. Now the values of $[HCO_3^-]_f$ can be calculated from eq 3. The plot of $[HCO_3^-]_f$ versus $(A_0 - A_e)$ can be constructed. The slope of this plot gives the buffer factor $Q_0{}^h$.

The effect of pressure on K_{HB} and K_1 must be considered. $\Delta\bar{V}$ for the ionization of Taps buffer is 0.5 ± 0.2 cm^3 mol^{-1},[57] which is the lowest value among several buffers. Therefore, the pressure effect on the ionization of Taps is sufficiently small that it can safely be neglected. The overall volume change for reaction 1 has been reported as −24.7 cm^3 mol^{-1} at 0.5 M NaCl.[48] Thus the value of K_1 at different pressures can be estimated using the relationship embodied in eq 4:

$$\left(\frac{d\ln K_1}{dP}\right)_T = \frac{24.7\ cm^3/mol}{RT} \quad (4)$$

At 25.0 °C eq 4 can be rewritten as

$$\ln K_1 = \ln K_1{}^0 + 0.010P \quad (5)$$

where K_1 and $K_1{}^0$ are the values at pressures P (MPa) and at ambient pressure, respectively. Thus K_1 at different pressures can be obtained from eq 5.

For the dehydration reaction eq 6 is used to calculate the extent of dehydration for any initial HCO_3^- concentration. Mes

$$[HCO_3^-]_0 = [CO_2]_f + \frac{K_1([B]_0 + [CO_2]_f)[CO_2]_f}{K_{HB}([HB^+]_0 - [CO_2]_f)} \quad (6)$$

buffer, for which the reaction volume of ionization is 3.9 ± 0.1 cm^3 mol^{-1},[57] was chosen for study of the dehydration reaction. The K_{HB} values at different pressures were calculated therefore based on eq 7, where K_{HB} and $K_{HB}{}^0$ are the equilibrium

$$\ln\frac{K_{HB}}{K_{HB}{}^0} = -1.573 \times 10^{-3}P \quad (7)$$

constant values at elevated pressures (in MPa) and ambient pressure respectively. p$K_{HB}{}^0$ and p$K_{DB}{}^0$ were determined to be 6.01 and 6.56 at 25 °C and 0.2 M ionic strength, respectively. For the calculation of K_1 at different pressures eq 5 is used.

Now the magnitude of the $[CO_2]_f$ can be calculated from eq 6. The plot of $[CO_2]_f$ versus $(A_0 - A_e)$ can be constructed. The slope of this plot yields the buffer factor Q_0[d].

Measurement of Isotope Effects. The heavy water experiments were carried out in a manner similar to that described above. Commercial standard buffers were used for calibration of the electrode. pD measurements in D_2O systems were made by the same pH meter, and then making the recommended addition of 0.40 pH units to correct the electrode readings in heavy water.[12] The electrode was rinsed several times with D_2O before a pD measurement was made. The corrections for K_1 and K_{DB} at different pressures in D_2O were made in a similar way as for H_2O as solvent.

Buffer Selection. The Taps buffer, suitable for biochemical reactions, was chosen for the hydration study because the pH of 8.6 for the reaction medium is close to the pK_a of Taps. At and near a pH of 8.6, hydration to HCO_3^- is virtually complete with little subsequent reaction to produce CO_3^{2-}.[56] Thus the total absorbance change is related to 1 released mol of protons/mol of CO_2; consequently the buffer factor can be obtained accurately. The ratio of $[B]/[HB^+]$ at a pH of 8.6 is such that the concentration of the basic form is double that of the acidic form so that at early reaction times the dehydration of HCO_3^- involving reaction of the protonated buffer with the enzyme is relatively unimportant. The buffer (Taps) catalyzed spontaneous hydration reaction rate is relatively small compared with other buffers used in biological reactions.[56] A further advantage of Taps buffer in the context of this study is the small volume change for proton ionization (vide supra). At the pH of measurement (8.6) the enzyme catalyzed CO_2 hydration kinetic parameters k^h_{cat} and k^h_{cat}/K^h_m are in the pH-independent range.[11,50,51,53] For the dehydration of HCO_3^-, the requirement that k^d_{cat} and k^d_{cat}/K^d_m be determined in the pH-independent region dictates the measurement range. The pK_a of 6.01 for Mes buffer places it in the satisfactory range. However, at a pH of 6.0 the dehydration reaction is not complete. The release of OH^- is the cause of the observed absorbance change. For the dehydration reaction the volume change due to proton ionization of Mes buffer, 3.9 $cm^3\ mol^{-1}$, cannot be ignored. However, this latter influence and the incomplete dehydration reaction can both be accounted for by the buffer factor obtained directly from kinetic traces.

Results

In anticipation of conducting high-pressure kinetics experiments, it was necessary to consider whether subjecting the enzyme in solution to high pressure would have any consequences beyond a kinetic one. A solution of a sample of HCA II was subjected to different pressures up to 150 MPa, and the UV spectra were recorded. No detectable differences in the spectra were observed. The activity of HCA II at atmospheric pressure before and after pressurizing up to 100 MPa was measured. No evident difference in activity was found.

Pressure Dependence of the CO_2 Hydration Reaction. To be able to obtain appropriate and correct experimental conditions for the measurements at high pressure, we remeasured kinetic data at ambient pressure according to the method described in the literature:[53] the dependence of the initial rate of CO_2 hydration on [B] in the presence and absence of HCA II at high $[CO_2]$ (supplementary Figure 1a), at low $[CO_2]$ (supplementary Figure 2a) and the dependence of initial rate of CO_2 hydration on $[CO_2]$ at high [B] (supplementary Figure 3a). The uncatalyzed rate was never more than 6% of the catalyzed hydration rate and since the magnitude of the former rate fell within the error range of the latter rate measurements, and considering the inherent error of the method, reaction not due to HCA II can be neglected. The results showed that at $[B] \leq 13$ mM, the rate-determining step is intermolecular proton transfer, and at $[B] > 20$ mM, the reaction becomes independent of [B], i.e., intramolecular proton transfer becomes rate-determining. These findings are similar to those of Rowlett and Silverman.[53] The pertinent reaction is shown in eq 8.

$$^+HE{\equiv}ZnOH^+ + B \underset{k_{-5}}{\overset{k_5}{\rightleftharpoons}} E{\equiv}ZnOH^+ + HB^+ \qquad (8)$$

The kinetic equation corresponding to this process has been shown to be (9).[53]

$$\frac{[E]}{v} = \frac{1}{k_5[B]} + \frac{1}{k^h_{cat}}\left(1 + \frac{K^h_m}{[CO_2]}\right) \qquad (9)$$

Values for k_5 of $(3.5 \pm 0.1) \times 10^8\ M^{-1}\ s^{-1}$ and $(2.6 \pm 0.6) \times 10^8\ M^{-1}\ s^{-1}$ from the dependence on [B] at high and low $[CO_2]$, respectively, and values for k^h_{cat} of $(8.1 \pm 0.9) \times 10^5\ s^{-1}$ and k^h_{cat}/K^h_m of $0.93 \times 10^8\ M^{-1}\ s^{-1}$ from the dependence on $[CO_2]$ at high [B], were obtained. These values are in good agreement with data reported by others[14,53] (summarized in supplementary Table I). Thus the pressure dependence of the intermolecular proton-transfer step can be studied at $[B] < 10$ mM. The pressure dependence of k^h_{cat}/K^h_m can be studied at $[CO_2] < 4$ mM, which is in the $[CO_2]$-dependent range, and at $[B] > 10$ mM, which is in the [B]-independent range. The pressure dependence of k^h_{cat} can be studied at $[CO_2] = 16.9$ mM, which is in the $[CO_2]$-independent range, and at $[B] > 10$ mM, which is in the [B]-independent range (see supplementary Figures 2 and 3).

The pressure dependences of k^h_{cat} and k_5 were studied under the conditions indicated. Some typical reaction traces are shown in Figure 1. The curves obtained at different pressures show similar initial slopes at both low and high buffer concentrations. The k^h_{cat} values derived from them (supplementary Table II) and the plot of ln k^h_{cat} versus pressure (supplementary Figure 4) showed that this parameter is pressure independent. This in turn implies that $\Delta V^{\ddagger}$ (for k^h_{cat}), measured at high buffer concentration and $\Delta V^{\ddagger}$ (for k_5) measured at low buffer concentration, are indistinguishable from zero.

The pressure dependence of k^h_{cat}/K^h_m was studied under the conditions described above (supplementary Table III). Typical plots of $\ln(k^h_{cat}/K^h_m)$ versus pressure are shown in Figure 2 at high buffer concentration (and in supplementary Figure 5 at low buffer concentration). From such plots the activation volumes were obtained and are listed in Table 1. At low buffer concentrations, the apparent value of $\Delta V^{\ddagger}$ is indistinguishable from zero, and with increase in buffer concentration its value becomes progressively negative and levels off to a common value, close to $-9\ cm^3\ mol^{-1}$, when the buffer concentration is 10 mM or higher. As pointed out above, the pressure dependence of k^h_{cat}/K^h_m can be measured only at a buffer concentration higher than 10 mM. The data shown here indicate that a reliable $\Delta V^{\ddagger}$ for k^h_{cat}/K^h_m of $-9\ cm^3\ mol^{-1}$ can be obtained.

Pressure Dependence of the HCO_3^- Dehydration Reaction. To select the experimental conditions for the study of the pressure dependence of the dehydration reaction, it was necessary to remeasure the kinetic parameters at ambient pressure. The initial reaction rate of dehydration was measured in the presence and absence of HCA II, using values for $[HCO_3^-]$ of 0.010 and 0.140 M for the low and high concentration studies, respectively. The results obtained at 0.010 and

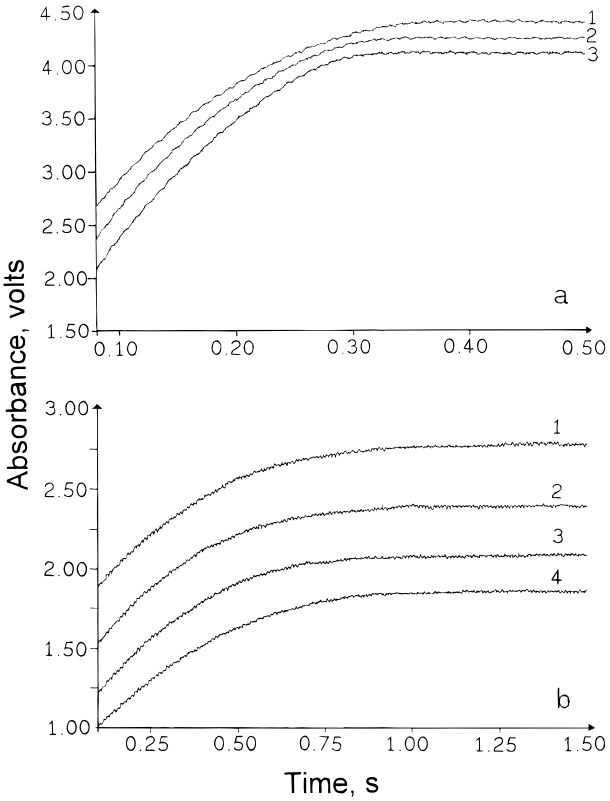

Figure 1. Typical kinetic traces of the CO_2 hydration reaction run under different pressures in both the [B]-dependent and the [B]-independent regions. Absorbance scale: 10 V = 1 unit of absorbance. Experimental conditions: $T = 25.0 \pm 0.1$ °C; ionic strength = 0.2 M (Na_2SO_4); pH (before reaction) = 8.62; pH (after reaction) = 5.96 for (a) and 8.47 for (b); [*m*-cresol purple] = 105 μM; [CO_2] = 16.9 mM; [HCA II] = 95 nM; [EDTA] = 10 μM; λ = 436 nm. Key: (a) $[Taps]_T$ = 5.0 mM, [B] = 3.2 mM; (b) $[Taps]_T$ = 50 mM, [B] = 32 mM. Curves 1, 2, 3, and 4 correspond to the pressures of 10, 50, 100, and 130 MPa. Curves were vertically separated for clarity.

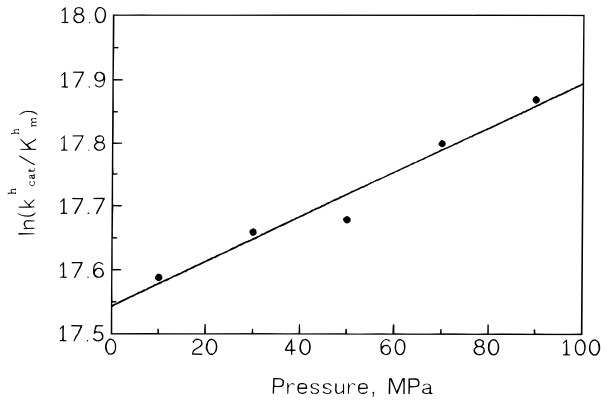

Figure 2. Plot of $\ln(k^h_{cat}/K^h_m)$ on pressure in the [B]-independent region. Experimental conditions: $T = 25.0 \pm 0.1$ °C; ionic strength = 0.2 M (Na_2SO_4); pH (before reaction) = 8.56; pH (after reaction) = 8.28−8.56; [*m*-cresol purple] = 41.8 μM; [HCA II] = 70 nM; [EDTA] = 10 μM; λ = 436 nm; $[Taps]_T$ = 15.0 mM; [B] = 9.36 mM.

0.140 M HCO_3^- are shown in supplementary Figures 6 and 7, respectively. Results similar to those in the literature[14] were found: the catalyzed dehydration rate increases with increase in $[HB^+]$ at concentrations below 10 mM, but becomes independent of $[HB^+]$ at concentrations above 10 mM. The spontaneous reaction is more than 10% of the catalyzed rate. The dependence of the initial rate of HCO_3^- dehydration upon $[HCO_3^-]$ at high $[HB^+]$ in the presence and absence of HCA II was also measured (supplementary Figure 8). Values for k^d_{cat} of $(2.2 \pm 0.1) \times 10^5$ s^{-1} and for k^d_{cat}/K^d_m of $(5.8 \pm 0.1) \times 10^6$ M^{-1} s^{-1} were obtained. At $[HCO_3^-] < 0.02$ M, the initial rate increases linearly with increasing $[HCO_3^-]$, and above 0.10 M, the initial rate is independent of $[HCO_3^-]$. The uncatalyzed rate can approach 26% of the catalyzed rate, and therefore correction of the catalyzed rate is necessary. Thus the pressure dependence of k^d_{cat}/K^d_m may be measured in the $[HCO_3^-]$-dependent range of 0.2−20 mM. For the pressure dependence of the turnover number, k^d_{cat}, the $[HCO_3^-]$-independent range of 0.10−0.175 M may be used. Since $NaHCO_3$ contains a significant amount of CO_2,[13] the hydration reaction of CO_2 could interfere with the dehydration measurement. Therefore corrections to the dehydration reaction rate were performed using the method described in the literature.[13] The correction to K^d_m is 3.7% and to k^d_{cat} is approximately 3%. Thus within the error range of the methods these correction factors do not need to be included.

TABLE 1: Activation Volumes, $\Delta V_1^{\ddagger}$ (cm^3 mol^{-1}), for k^h_{cat}/K^h_m at Different Buffer Concentrations[a]

[B], mM	5.78	7.68	9.63	9.63	19.3	32.0
$\Delta V_1^{\ddagger}$	-1.1 ± 2	-3.3 ± 2.3	-8.0 ± 1.5	-8.7 ± 1.0	-9 ± 3	-9 ± 1
γ[b]	0.359	0.709	0.967	0.979	0.905	0.995

[a] Experimental conditions: $T = 25.0 \pm 0.1$ °C; $[B]/([HB^+] + [B]) = 0.64$; ionic strength = 0.2 M (Na_2SO_4); [*m*-cresol purple] = 41.8 μM; [HCA II] = 70 nM; [EDTA] = 10 μM; pH (before reaction) = 8.75 ± 0.05. A weighted linear-squares method with V^4 weights was used to obtain k^h_{cat}/K^h_m. [b] Correlation coefficient.

The catalyzed and uncatalyzed dehydration reactions were monitored kinetically under the conditions selected above. Typical reaction traces for the HCO_3^- dehydration reaction at low and high $[HCO_3^-]$ as a function of pressure are shown in Figure 3. The initial slopes show a trend of decrease in rate with increase in pressure, in both cases. The catalyzed rates were obtained by subtracting the uncatalyzed rates from the apparent catalyzed rates. The derived values of k^d_{cat}, k^d_{cat}/K^d_m, and k^d ($=v^d_{initial}/([H^+][HCO_3^-])$[56]) measured in H_2O and D_2O at different pressures are listed in supplementary Table IV. The plots of the natural log of the derived kinetic parameters versus pressure are shown in Figures 4 and 5, respectively, and from them the values of $\Delta V^{\ddagger}$ for k^d_{cat}/K^d_m and k^d_{cat} were obtained. These results are summarized in Table 2.

Discussion

Correlations between the Kinetic Parameters, k^h_{cat}, k^h_{cat}/K^h_m, k^d_{cat}, and k^d_{cat}/K^d_m and Specific Steps in the Proposed Mechanism. To assign the measured activation parameters to discrete steps in the mechanism, it is necessary to consider the kinetic equations describing the catalytic cycle in more detail.

The steady state rate equation contains a complicated set of terms involving both substrate and buffer concentrations. However, at high buffer concentrations, step 5 is effectively an equilibrium process,[15] and the buffer concentration can be omitted. The rate equation takes the form shown in eq 10 with the terms defined as in the literature,[15] where $v_{ss} = -d[CO_2]/dt = d[HCO_3^-]/dt$.

$$\frac{v_{ss}}{[E]_t} = \frac{(k^h_{cat}/K^h_m)[CO_2] - (k^d_{cat}/K^d_m)[HCO_3^-]}{1 + [CO_2]/K^h_m + [HCO_3^-]/K^d_m + [CO_2][HCO_3^-]/K_{hd}} \quad (10)$$

The steady-state reaction rate v_{ss} is a measurable parameter applicable to an equilibrium condition, and the relevant equi-

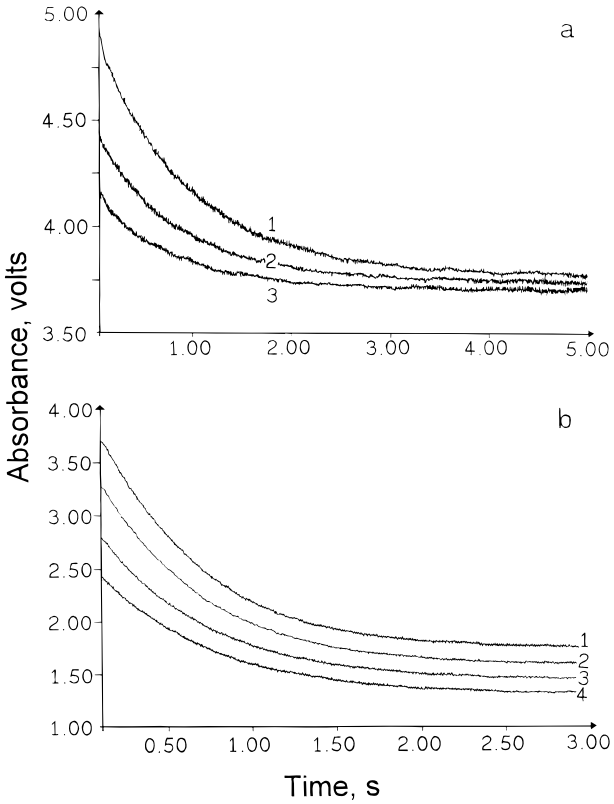

Figure 3. Typical kinetic traces for the HCO_3^- dehydration reaction run under different pressures in both the [HCO_3^-]-dependent and in the [HCO_3^-]-independent regions. Absorbance scale: 10 V = 1 unit of absorbance. Experimental conditions: $T = 25.0 \pm 0.1$ °C; ionic strength = 0.2 M (Na_2SO_4); pH (before reaction) = 6.17; pH (after reaction) = 6.62 at low [HCO_3^-] (see a) and 7.53 at high [HCO_3^-] (see b); [bromocresol purple] = 35.7 μM; [HCA II] = 80 nM; [EDTA] = 10 μM; λ = 420 nm. Key: (a) [HCO_3^-] = 8.0 mM, curves 1, 2, and 3 correspond to pressures of 10, 75, and 130 MPa; (b)[HCO_3^-] = 150 mM, curves 1, 2, 3, and 4 correspond to pressures of 10, 45, 75, and 100 MPa, respectively. Curves were vertically separated for clarity.

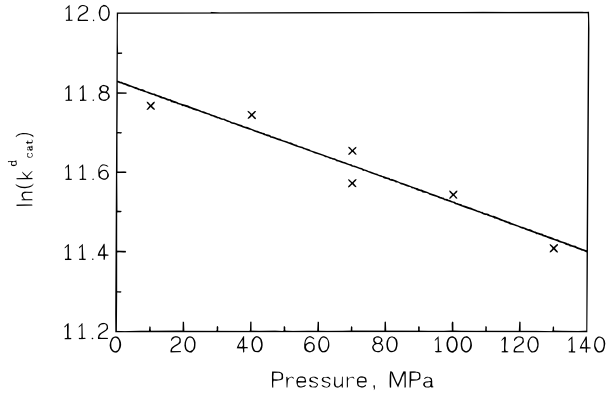

Figure 4. Plot of $\ln(k^d_{cat})$ versus pressure in the [HB^+]-independent region. Experimental conditions: $T = 25.0 \pm 0.1$ °C; ionic strength = 0.2 M (Na_2SO_4); pH (before reaction) = 6.17; pH (after reaction) = 7.53; [HCO_3^-] = 150 mM; [bromocresol purple] = 35.7 μM; [HCA II] = 80 nM; [EDTA] = 10 μM; λ = 420 nm; $[Mes]_T$ = 30 mM; [HB^+] = 12.4−13.8 mM (depending on the pressure).

librium equation contains both reactant and product terms. When the reaction is far from the equilibrium position, exclusion of any of the product terms is still not permitted. When using the pH indicator method,[50] only initial rates can be measured. It is a satisfactory and common practice in treating initial rate data that all product terms can be eliminated.[58] Considering the fact that all conclusions could be drawn based on the initial rate data using the pH indicator method,[13,31,50,53] such an approximation can also be used here. Therefore, when only the hydration reaction is concerned, all terms containing [HCO_3^-] can be omitted, and eq 10 reduces to eq 11, which can also be deduced eventually from eq 9 at high buffer concentration.

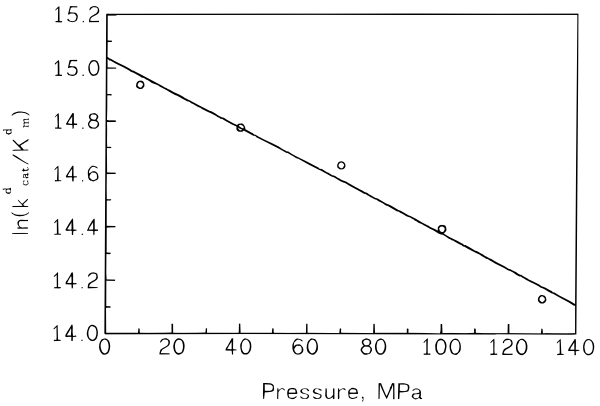

Figure 5. Plot of $\ln(k^d_{cat}/K^d_{cat})$ versus pressure in the [HB^+]-independent region. Experimental conditions: $T = 25.0 \pm 0.1$ °C; ionic strength = 0.2 M (Na_2SO_4); pH (before reaction) = 6.17; pH (after reaction) = 6.62; [HCO_3^-] = 8.0 mM; [bromocresol purple] = 35.7 μM; [HCA II] = 80 nM; [EDTA] = 10 μM; λ = 420 nm; $[Mes]_T$ = 30 mM; [HB^+] = 12.4−13.8 mM (depending on the pressure).

TABLE 2: Activation Volumes $\Delta V^‡$ for k^d_{cat}, k^d_{cat}/K^d_m, and k^d in H_2O[a] and D_2O[b]

pH or pD	$\Delta V^‡$ (k^d_{cat}) (cm^3 mol^{-1})	$\Delta V^‡$ (k^d_{cat}/K^d_m) (cm^3 mol^{-1})	$\Delta V^‡$ (k^d) (cm^3 mol^{-1})
6.17 (H_2O)	+9 ± 1	+14.7 ± 1.2	+13.7 ± 0.8
6.83 (D_2O)	+10 ± 3		+10.4 ± 0.5
5.66 (H_2O)		+13.2 ± 2.1[c]	

[a] Experimental conditions: $T = 25.0 \pm 0.1$ °C; ionic strength = 0.2 M (Na_2SO_4); $[Mes]_T$ = 30 mM; [EDTA] = 10 μM; [HCA II] = 80 nM; [bromocresol purple] = 30.7 μM; [HCO_3^-] = 0.0080 M for the measurement of k^d_{cat}/K^d_m and 0.150 M for the measurement of k^d_{cat}. pH (before reaction) = 6.17; pH (after reaction) = 6.62 and 7.53 for [HCO_3^-] of 0.0080 and 0.150 M, respectively. [b] Experimental conditions are the same as above except for the following: [HCA II] = 97.3 nM; [bromocresol purple] = 30 μM; [HCO_3^-] = 0.150 M; pD (before reaction) = 6.83; pD (after reaction) = 7.84. [c] Experimental conditions are the same as in footnote *a* except for the following: pH (before reaction) = 5.66; pH (after reaction) = 6.10 and 6.87 for [HCO_3^-] of 0.0080 and 0.150 M, respectively.

$$\frac{v^h_{initial}}{[E]_t} = \frac{k^h_{cat}/K^h_m[CO_2]}{1 + [CO_2]/K^h_m} \tag{11}$$

where

$$k^h_{cat} = \frac{k_2k_3k_4}{k_2k_3(1 + [H^+]/K_{E2}) + k_4(k_2 + k_3)} \tag{12}$$

and

$$\frac{k^h_{cat}}{K^h_m} = \frac{k_1}{1 + [H^+]/K_{E1}} \tag{13}$$

In eqs 12 and 13, K_{E1} (=$[H^+][E{\equiv}ZnOH^+]/[E{\equiv}Zn(H_2O)^{2+}]$) is the acid dissociation constant of the catalytic group related to coordinated H_2O[40] and K_{E2} (=$[H^+][E{\equiv}ZnOH^+]/[^+HE{\equiv}ZnOH^+]$) is the acid dissociation constant of the proton-transfer group related to His-64.[18] The value of pK_{E1} is close to 6.8[50] and the magnitude of pK_{E2} is close to 7.6.[53] The kinetics were followed at a pH above 8.6, then since $[H^+] \ll K_{E1}$, K_{E2}, eqs 12 and 13 reduce respectively to eqs 14 and 15.

$$k^{h}_{cat} = \frac{k_2k_3k_4}{k_2k_3 + k_4(k_2 + k_3)} \quad (14)$$

$$\frac{k^{h}_{cat}}{K^{h}_{m}} = k_1 \quad (15)$$

When the intramolecular proton-transfer step is rate-limiting at high buffer concentration, then (14) becomes eq 16, since $k_4 \ll k_2$ and k_3.

$$k^{h}_{cat} = k_4 \quad (16)$$

Thus at high buffer concentrations the turnover number is the rate constant for intramolecular proton transfer, k_4.

In considering the reverse reaction, $[CO_2]$ is the product term. Using a parallel approximation as was used for the hydration reaction, all $[CO_2]$-containing terms in eq 10 can be eliminated and eq 17 results

$$\frac{v^{d}_{initial}}{[E]_t} = \frac{k^{d}_{cat}/K^{d}_{m}[HCO_3^-]}{1 + [HCO_3^-]/K^{d}_{m}} \quad (17)$$

where

$$k^{d}_{cat} = \frac{k_{-1}k_{-2}k_{-4}}{k_{-1}k_{-2}(1 + K_{E2}/[H^+]) + k_{-4}(k_{-1} + k_{-2})} \quad (18)$$

and

$$\frac{k^{d}_{cat}}{K^{d}_{m}} = \frac{k_{-3}k_{-4}}{k_4(K_{E2}/[H^+])(1+[H^+]/K_{E1})} \quad (19)$$

where K_{E1} and K_{E2} retain their definition, and it is noted that $k_4/k_{-4} = K_{E1}/K_{E2}$. Then eq 19 reduces to

$$\frac{k^{d}_{cat}}{K^{d}_{m}} = \frac{k_{-3}[H^+]}{[H^+] + K_{E1}} \quad (20)$$

The experimental conditions were chosen such that $[H^+] \gg K_{E1}$, K_{E2}, then eqs 18 and 20 reduce to eqs 21 and 22, respectively.

$$k^{d}_{cat} = \frac{k_{-1}k_{-2}k_{-4}}{k_{-1}k_{-2} + k_{-4}(k_{-1} + k_{-2})} \quad (21)$$

$$\frac{k^{d}_{cat}}{K^{d}_{m}} = k_{-3} \quad (22)$$

Equation 22 illustrates that the operational rate constant k^{d}_{cat}/K^{d}_{m} under the conditions reported is equal to the rate constant k_{-3}, for the replacement of the Zn^{2+} coordinated water by the HCO_3^-. A simplification of eq 21, similar to that which was carried out for the hydration reaction (eq 14 converted to eq 16), is not justifiable for the dehydration reaction, as can be seen from the following. The hydrogen/deuterium isotope effect on k^{d}_{cat} as well as on k^{h}_{cat} of 3.8 obtained from solvent substitution (D_2O for H_2O) indicated that a primary isotope effect, on one reaction step involving transfer of hydrogen, is probably dominating.[13] The comparative studies of bovine carbonic anhydrase in H_2O and D_2O showed that[51] the effect on k^{d}_{cat} is 3.3 at the basic plateau, while the effect on k^{h}_{cat} is 4.3 at the acidic plateau. These revealed the importance of a primary intramolecular proton transfer for both hydration and dehydration reaction in the catalysis. In addition it has been shown[15] that the ^{13}C exchange between CO_2 and HCO_3^- is faster than the maximal rate constants in either direction and furthermore is independent of buffer concentration and has no hydrogen/deuterium isotope effect. This was interpreted as evidence for a prior rate-determining proton transfer (k_{-4}), separate from the exchange process. However, our value of $\Delta V^{\ddagger}$ of (8.5 ± 1.3) cm^3 mol^{-1} is not readily reconciled with these earlier findings. In the present study, the solvent kinetic isotope effects of 3.6 ± 1.4 were found over the pressure range from 10−100 MPa. The activation volumes of 9 ± 1 in H_2O and 10 ± 3 cm^3 mol^{-1} in D_2O solution are similar. Since $\Delta V^{\ddagger}$ is expected to be close to zero for proton transfer, k_{-2} and k_{-4} (see further discussion), these results indicate that CO_2 release (k_{-1}) most probably accounts for the observed pressure effect, whereas the isotope effect resides in k_{-4}.

TABLE 3: Summary of Activation Volumes for Individual Steps Outlined in Scheme 2

	$\Delta V^{\ddagger}$, cm^3 mol^{-1}		
k_1	−9 ± 1	k_{-1}	+9 ± 1
k_2	zero	k_{-2}	zero
k_3	+6.0 ± 0.6[a]	k_{-3}	+14.0 ± 1.2
k_4	zero	k_{-4}	zero
k_5	zero	k_{-5}	zero

[a] Calculated from eq 24.

Activation Volumes and Volume Profile. On the basis of the above correlations between the kinetic parameters and specific steps in the proposed mechanism, the activation volumes obtained for the kinetic parameters (see Tables 1 and 2) can be assigned to the activation volumes for the individual steps outlined in the Scheme 2. The results are summarized in Table 3.

Under the limiting conditions for eqs 15 and 16, $\Delta V^{\ddagger}(k_1) = -9 \pm 1$ cm^3 mol^{-1} and $\Delta V^{\ddagger}(k_4) \sim 0$ for the hydration of CO_2. It is noteworthy that the activation entropies reported for these steps follow a parallel trend, viz. −18.7 and −3.99 cal mol^{-1} K^{-1} for k_1 and k_4, respectively.[16] In other words k_1 and k_4 are associated respectively with increasing molecular ordering and similar molecular ordering upon achieving the transition state, as expected. According to the results in Table 2, the dehydration of HCO_3^- is characterized by the mean values $\Delta V^{\ddagger}(k_{-3}) = +14.0 \pm 1.2$ and $\Delta V^{\ddagger}(k_{-1}k_{-2}/(k_{-1} + k_{-2})) = +9 \pm 1$ cm^3 mol^{-1} in H_2O and 10 ± 3 cm^3 mol^{-1} in D_2O under the limiting conditions of eq 22. The latter value of $\Delta V^{\ddagger}(k^{d}_{cat})$, where $k^{d}_{cat} = k_{-1}k_{-2}/(k_{-1} + k_{-2})$, may be further analyzed: the observed isotope effect on the value of k^{d}_{cat}, can be assigned to the effect on k_{-2}; and the observed $\Delta V^{\ddagger}(k^{d}_{cat})$ value of +9 ± 1 cm^3 mol^{-1} can be assigned to the release of CO_2. On decreasing the pH from 6.17 to 5.66 (see Table 2), there is no significant effect on $\Delta V^{\ddagger}$ for k^{d}_{cat}/K^{d}_{m}. This means that K_{E1}, which contributes significantly to the magnitude of k^{d}_{cat}/K^{d}_{m} at lower $[H^+]$, according to eq 22, does not exhibit a meaningful pressure dependence and it is safe to conclude that $\Delta\bar{V}(K_{E1}) \approx 0$. Thus the deprotonation of coordinated water does not cause a significant change in volume. A similar behavior is expected for the deprotonation of His 64 expressed by K_{E2}, from which it follows that k_4/k_{-4} ($=K_{E1}/K_{E2}$) should also be independent of pressure. Combined with our observation that k_4 is independent of pressure, we can then conclude that k_{-4} must also be independent of pressure. Alternatively, if we consider the species $E{\equiv}ZnOH_2^{2+}$ and $^{+}HE{\equiv}ZnOH^{+}$ in Scheme 2, it is reasonable to expect that their partial molar volumes will be very similar, i.e., $\Delta\bar{V}(K_4) \approx 0$, from which it can be concluded again that $\Delta V^{\ddagger}(k_{-4}) = \Delta V^{\ddagger}(k_4) \approx 0$. Thus the observed pressure

SCHEME 3

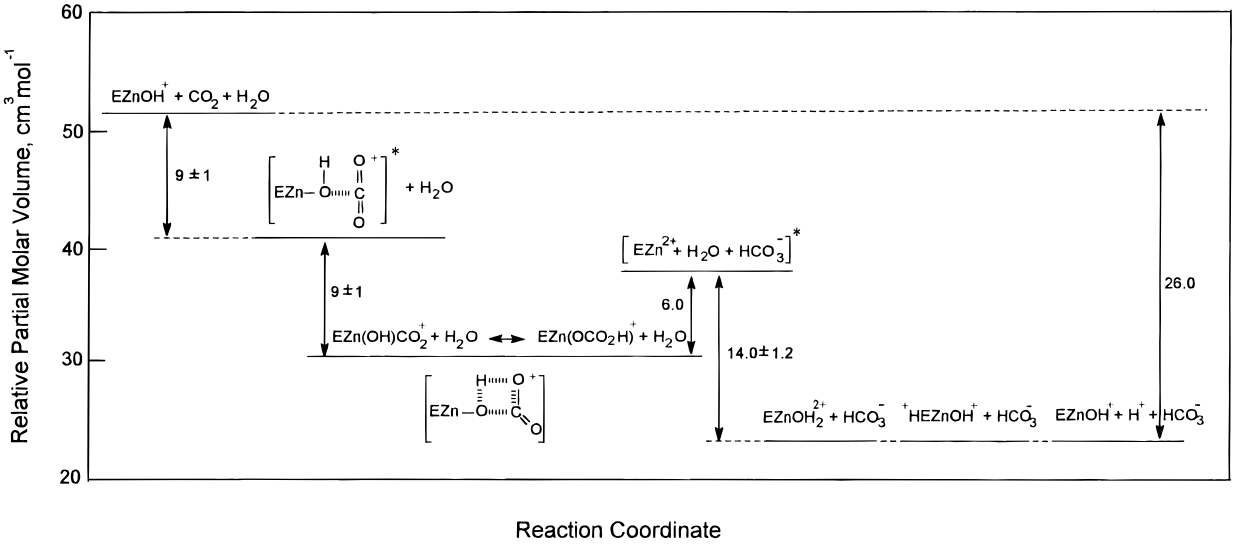

dependence of k^{d}_{cat} must be due to the effect of pressure on k_{-1}, i.e., the release of CO_2 will be accompanied by a volume increase.

One way of testing the validity of kinetic data is to compare forward and reverse kinetics within Haldane relationships:[13]

$$\frac{k^{h}_{cat}}{K^{h}_{m}}\frac{K^{d}_{m}}{k^{d}_{cat}}K_{E2} = K_{eq} \qquad (23)$$

where K_{eq} is the equilibrium constant of eq 1. The pressure effect on the forward and reverse reactions should be equal to the pressure effect on the overall reaction. The pressure effect on the forward and reverse reaction is $\Delta V^{\ddagger}(k^{h}_{cat}/K^{h}_{m}) - \Delta V^{\ddagger}(k^{d}_{cat}/K^{d}_{m}) + \Delta\bar{V}(K_{E2}) = -9 - (+14) + 0 = -23$ cm^3 mol^{-1}. The overall reaction volume for eq 1 has been reported to be -26.9 cm^3 mol^{-1} at zero ionic strength[48] and -23.7 cm^3 mol^{-1} at 0.725 M ionic strength.[59] By employing a linear interpolation, these values result in a reaction volume of -26.0 cm^3 mol^{-1} at 0.2 M ionic strength and 25 °C. Therefore our activation volumes obtained are very reasonable in the context of Haldane relationships.

These $\Delta V^{\ddagger}$ values enable us to construct an overall volume profile for the reaction steps outlined in Scheme 2 if a value for $\Delta V^{\ddagger}$ ($=\Delta V^{\ddagger}_{3}$) can be obtained. By using the overall volume change of eq 1, -26.0 cm^3 mol^{-1}, it is possible to estimate $\Delta V^{\ddagger}_{3}$ from eq 24.

$$\begin{aligned}\Delta V^{\ddagger}_{3} &= \Delta\bar{V}_{3} + \Delta V^{\ddagger}_{-3}\\ &= \Delta\bar{V} - \Delta\bar{V}_{1} - \Delta\bar{V}_{2} - \Delta\bar{V}_{4} - \Delta\bar{V}_{5} + \Delta V^{\ddagger}_{-3}\\ &= \Delta\bar{V} - (\Delta V^{\ddagger}_{1} - \Delta V^{\ddagger}_{-1}) - \Delta\bar{V}_{2} - \Delta\bar{V}_{4} - \Delta\bar{V}_{5} + \Delta V^{\ddagger}_{-3}\\ &= (-26.0 + 9 + 9 - 0 - 0 - 0 + 14.0)\ \text{cm}^3\ \text{mol}^{-1}\\ &= +6.0\ \text{cm}^3\ \text{mol}^{-1} \qquad (24)\end{aligned}$$

The volume profile obtained is presented in Scheme 3. The first step involves nucleophilic attack of E≡ZnOH$^+$ on CO_2 to produce E≡Zn(OH)CO_2^+. The partial molar volume of the transition state lies almost halfway between that of the reactant and product states. The overall volume collapse for the catalyzed CO_2 uptake reaction of 18 cm^3 mol^{-1} ($+9 + 9$ cm^3 mol^{-1}) is consistent with the volume change of binding of CO_2 to the coordinated hydroxo ligand. By way of comparison, the volume profile for the spontaneous hydration of CO_2 is characterized by a volume collapse of 10.8 ± 1.9 cm^3 mol^{-1} to reach the transition state, followed by a further volume decrease of 6.4 ± 0.4 cm^3 mol^{-1} to produce H_2CO_3, i.e., an overall volume decrease of 17 ± 2 cm^3 mol^{-1}. Deprotonation of H_2CO_3 is characterized by a further volume decrease of 8.4 ± 0.1 cm^3 mol^{-1},[48] which results in an overall reaction volume of -25.6 ± 1.4 cm^3 mol^{-1}. The value of $\Delta V^{\ddagger}(k^{d})$ reported for the uncatalyzed dehydration of HCO_3^-, viz., $+13.7 \pm 0.8$ cm^3 mol^{-1} (Table 2), in this study is in good agreement with the latter values, viz., $(+6.4 \pm 0.8) + (+8.4 \pm 0.1) = +14.8 \pm 0.8$ cm^3 mol^{-1}, and indicates a large volume increase during the process, $H^+ + HCO_3^- \rightarrow [H_2O\cdots CO_2]^{\ddagger}$. The similar value of $\Delta V^{\ddagger}(k^{d})$ (10.4 ± 0.5 cm^3 mol^{-1}) found in D_2O supports this suggestion. A solvent isotope effect on k^{d} of 0.61 ± 0.09 (H_2O/D_2O) at pressures up to 100 MPa was observed (see supplementary Table IV). Since a D−O bond is stronger than an H−O bond, the (D−)O−C bond will be weaker than the (H−)O−C bond. Consequently, a reaction involving C−O bond breakage in D_2O will be faster than in H_2O solution, which is in agreement with the observed secondary isotope effect. By way of a further comparison, the binding of CO_2 to $Co(NH_3)_5OH^{2+}$ to produce $Co(NH_3)_5OCO_2H^{2+}$ is characterized by a volume of activation of -10.1 ± 0.6 cm^3 mol^{-1} for the forward reation, and a value of $+6.8 \pm 0.3$ cm^3 mol^{-1} for the reverse decarboxylation reaction,[46] i.e., an overall reaction volume of -17 ± 1 cm^3 mol^{-1}. It follows that the volumes of activation for k_1 and k_{-1} and the reaction volume for K_1 in Scheme 2 are in close agreement with those observed for CO_2 uptake and decarboxylation in other systems.

The second step in Scheme 3 involves proton transfer from coordinated oxygen E≡Zn(OH)CO_2^+ to the uncoordinated oxygen E≡Zn(OCO_2H)$^+$. The partial molar volumes of the two species are expected to be very similar since there was essentially no difference in activation volumes in H_2O and D_2O solutions for the concerted steps of k_{-4} and k_{-1}. By way of comparison, $\Delta V^{\ddagger}$ for intramolecular exchange of bridging and terminal hydride ligands of H(μ-H)$Os_3(CO)_{10}(PPh_3)$ was also found to be close to zero.[60] The third step in Scheme 3 is the substitution of coordinated HCO_3^- by water. This reaction is characterized by a volume of activation of $+6.0 \pm 0.6$ cm^3 mol^{-1} for the forward and $+14.0 \pm 1.2$ cm^3 mol^{-1} for the reverse reactions, respectively. The reverse reaction involves the release of coordinated water, and the observed pressure dependence is such that it suggests the operation of a limiting

D mechanism. Theoretical calculations have predicted a maximum volume increase of 13 $cm^3\ mol^{-1}$ during the dissociation of a coordinated water molecule in terms of a dissociative mechanism.[61] The value observed for the dissociation of HCO_3^- is significantly smaller, but it should be kept in mind that this reaction involves an increase in charge. An increase in charge will cause volume reduction due to solvent restriction which will offset the overall volume increase and account for the observed trend.[1] On the basis of these arguments we conclude that ligand substitution (water for HCO_3^-) on the enzyme also follows a D mechanism. Complex-formation reactions of aquated Zn^{2+} are characterized by a $\Delta V^{\ddagger}$ value of $+6\ cm^3\ mol^{-1}$ and assigned to the operation of an I_d mechanism.[62] In the present case, however, labilization by the histidine ligands as well as the special ligand environment within the protein pocket may induce a changeover to a limiting D mechanism. The final steps in Scheme 3 involve proton transfer within the pocket of the active site, and no major volume changes are expected to be associated with this process, as outlined above. Deprotonation of coordinated water during which H^+ is released, or deprotonation of His-64 does not result in a meaningful volume change.

The volume profile in Scheme 3 and the observed pressure effects support the Zn^{2+}-hydroxide mechanism.[13] The mechanistic characteristics of steps 1 and 3 in Scheme 2 are in good agreement with those observed for model systems[46,48] and related systems in coordination chemistry. Our observation that CO_2 uptake and decarboxylation follow the expected trends is important. The bicarbonate for water substitution on Zn^{2+} in HCA II most probably follows a D mechansim, and not an I_d as would have been predicted on the basis of the coordination chemistry of aquated Zn^{2+}. Thus the special environment of the Zn^{2+} center induces a limiting D mechanism.

Mechanistic Insight from the Volume Profile Analysis. The volume profiles with respect to the CO_2 uptake (hydration) and release reaction (dehydration) for the HCA II catalyzed and the spontaneous reactions have comparable features. One can consider the principle that bond formation and bond breakage for both reactions may take place in a parallel way. A detailed reaction mechanism for the catalyzed reaction may be drawn as shown in Scheme 4, and the mechanism for the spontaneous reaction may be summarized as in Scheme 5. The latter is based partly on the volume profile obtained previously.[48] As shown in the scheme, two water molecules are suggested to participate in the spontaneous reaction. This two-water reaction mechanism is comparable to the catalyzed reaction in Scheme 4. One water molecule is the reactant, and the second is equivalent to the enzyme $E{\equiv}Zn^{2+}{-}OH^-$. Theoretical calculations[19] have shown that the two-water reaction mechanism is in better agreement with the experimental findings than a scheme involving only one water molecule. In these two schemes, the role of the OH^- (from the enzyme $E{\equiv}Zn^{2+}{-}OH^-$) for the catalyzed reaction is proposed to be, in a sense, equivalent to the role of the OH^- group (from H_2O) for the spontaneous reaction. This permits the following discussion.

(1) To proceed from 1 → 2, several proposals have been made. In the so-called outer-sphere mechanism[44] the oxygen of $E{\equiv}Zn^{2+}{-}OH^-$ directly attacks the carbon of CO_2. In another mechanism an oxygen of CO_2 coordinates with the Zn^{2+} center followed by a nucleophilic attack of the oxygen from the hydroxide ligand upon the carbon atom of CO_2 (inner-sphere mechanism[44]). Because similar activation volumes were found for reaching the transition states for 1 → 2 ($\Delta V^{\ddagger} = -9 \pm 1\ cm^3\ mol^{-1}$) and 1′ → 2′ ($\Delta V^{\ddagger} = -10.8 \pm 1.9\ cm^3\ mol^{-1}$), the O−C bond formation (O is from $E{\equiv}Zn^{2+}{-}OH^-$ for 1 → 2, and from H−O−H for 1′ → 2′) is proposed to take place via a similar addition mechanism. The formation of the Zn−O bond would be expected to result in a different value of $\Delta V^{\ddagger}$ for the catalyzed reaction as compared to the spontaneous reaction (only a C−O bond can be formed), since it will then involve a ligand substitution (O from CO_2 for O from coordinated OH^-) on the Zn^{2+} metal center. It therefore leads to the conclusion that the inner-sphere mechanism, in which a Zn−O bond is proposed to form, is not likely to occur, since by way of comparison there is no Zn^{2+} species available for the spontaneous reaction. Therefore our results favour the outer-sphere mechanism as shown in the schemes.

(2) For the formation of the bicarbonate intermediate, concerning $E{\equiv}Zn(OH)CO_2^+ \rightarrow E{\equiv}ZnOCO_2H^+$, two mechanisms have been proposed, namely, the Lipscomb mechanism[63] and the Lindskog mechanism.[44] In the former there is a proton

SCHEME 4

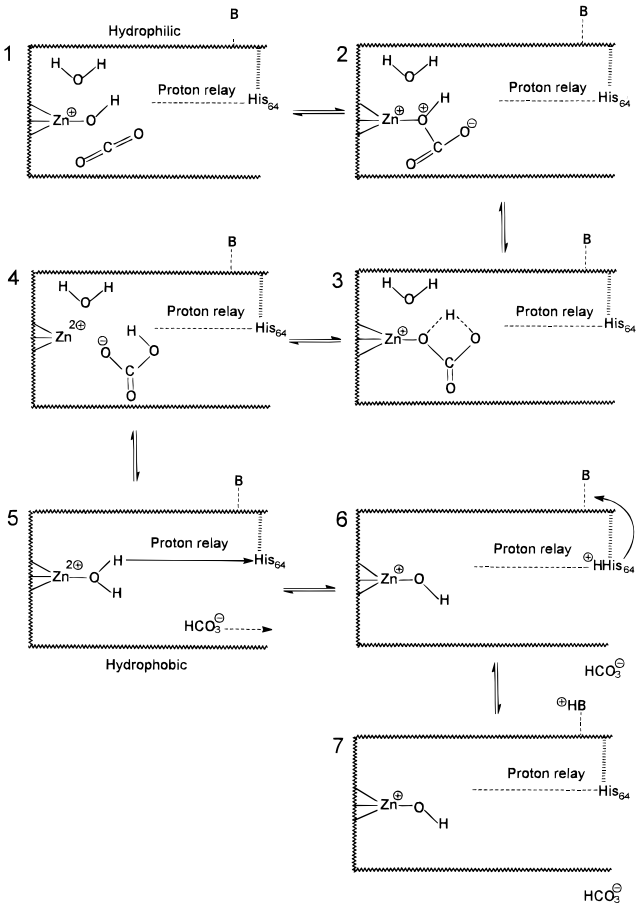

SCHEME 5

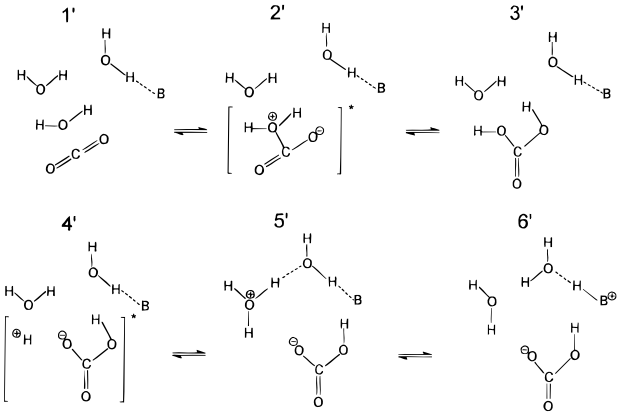

transfer between two oxygen atoms following the nucleophilic attack (1 → 2), whereas in the second mechanism there is no proton transfer but an oxygen atom directly coordinates to the Zn^{2+} center.[64] Theoretical calculations indicated that inclusion of environmental effects in the reaction coordinate are important in both mechanisms and are especially relevant in the case of the Lipscomb mechanism.[65] Recently, a correlation of the rate constants for decarboxylation reactions with those for the acid dissociation of coordinated bicarbonate[65] led to the suggestion that the rate-determining step for the decarboxylation reaction is the proton transfer from an uncoordinated oxygen atom to the coordinated oxygen atom of the carbonate ligand, i.e., $E{\equiv}ZnOCO_2H^+ \rightarrow E{\equiv}Zn(OH)CO_2^+$. Therefore, a similar mechanism for the CA-catalyzed reaction was predicted.[66] In a consistent manner with the spontaneous reaction mechanism (2′ → 3′), our findings favor the Lipscomb mechanism. However, the product $E{\equiv}ZnOCO_2H^+$ is not necessarily formed as a stable species during the forward reaction. A relatively stable species may be a hydrogen bridging bicarbonate intermediate (3) between $E{\equiv}Zn(OH)CO_2^+$ and $E{\equiv}ZnOCO_2H^+$ as shown in the volume profile (Scheme 3). When the substitution of HCO_3^- by H_2O occurs, the bridging proton labilizes the Zn−O bond ($E{\equiv}Zn{\cdots}OHCO_2^+$) and a substitution reaction occurs. When decarboxylation takes place, the bridging proton weakens the O−C bond ($E{\equiv}ZnHO{\cdots}CO_2^+$), and the release of CO_2 proceeds. When neither hydration of CO_2 nor dehydration of HCO_3^- are required physiologically, the hydrogen bridging bicarbonate intermediate is in an equilibrium between $E{\equiv}Zn(OH)CO_2^+$ and $E{\equiv}ZnOCO_2H^+$. This suggests that one essential function of the enzyme is its capability to maintain the proton of the coordinated bicarbonate on the oxygen atom coordinated to the metal center and this combination can labilize both Zn−O and C−O bonds, facilitating 3 → 4 and 2 → 1 respectively, depending on whether hydration of CO_2 or dehydration of HCO_3^- is required physiologically. Recently reported results are consistent with this mechanistic description.[66] Due to the absence of this environment, model complex catalyzed reactions and the spontaneous reaction proceed much more slowly than does the enzyme catalyzed reaction. Structural studies of the enzyme have indicated an environment suitable for the stabilization of such a configuration.[67]

(3) The nature of the bicarbonate intermediate has been discussed.[45] Is the bicarbonate ligand bound to the Zn^{2+} via only one (unidentate) or via two oxygen atoms (bidentate)? In the carbonate complex $[\{\eta^3\text{-HB(3,5-Pr}^i_2\text{pz)}_3\}Zn]_2(\mu\text{-}\eta^1,\eta^2\text{-}CO_3)$ the carbonate ligand bridges the two zinc centers in an asymmetric manner and is unidentate to one zinc center but bidentate to the other.[45] X-ray absorption data for carbonic anhydrase in the presence of bicarbonate suggests that the zinc center remains four-coordinated.[68] Studies on metal-substituted carbonic anhydrases[45] have revealed that the order of activity decreases along the series Zn > Co ≫ Ni ∼ Cu, which correlates with the tendency of these metals to favor bidentate coordination in model systems with nitrate ions.[45] The investigation of the catalytic activities, toward hydration of CO_2 and the dehydration of HCO_3^-, of Zn^{2+}−[12]aneN_3 and Zn^{2+}−[12]aneN_4 is also of relevance.[56,69] The former complex has a four-coordinate Zn^{2+} and the second one has a five-coordinate Zn^{2+} center. Beside that the two complexes are structurally and thermodynamically very similar. The five-coordinate Zn^{2+}−[12]aneN_4 was found to be much more reactive than the four-coordinate Zn^{2+}−[12]-aneN_3. For the five-coordinate complex, the bicarbonate intermediate cannot undergo a ring-closure reaction (formation of a bidentate bicarbonate intermediate), while for the four-coordinate complex, the bicarbonate intermediate has the chance to bind in a bidentate manner. Therefore it may be concluded that the chelation of coordinated bicarbonate slows the overall catalytic reaction,[69] and thus the claim that the bidentate bicarbonate formation inhibits the catalytic cycle is favored. Our results (intermediates 2 and 3), shown in Scheme 4, indicate a unidentate bicarbonate Zn^{2+} center, which is in agreement with these earlier findings.

In addition, the enzyme may disperse the positive charge from the Zn^{2+} center before the nucleophilic attack takes place. It is clear that the nucleophilicity of the hydroxide ligand of a +1 charged $Zn(OH)^+$ center cannot be greater than that of a neutral water H−O−H molecule. Theoretical calculations have shown that the nucleophilicity of a hydroxide ligand is inhibited by interaction with the bare Zn^{2+} cation in the gas phase.[20] Therefore, we assume that the enzyme may play a role in dispersing the positive charge of $E{\equiv}Zn^{2+}$ in order to cause the coordinated OH^- moiety to be sufficiently nucleophilic to attack CO_2. The groups to which the positive charge may be dispersed are likely to be aspartate or glutamate in the second shell,[21] because the pK_a values for them (approximately 4[70]) are such that the deprotonated forms are present in the neutral or slightly basic reaction medium. The possibility of ionizing a histidine in addition to water was also suggested.[71] Therefore, even coordinated histidine residues in the first shell may also carry part of the positive charge for a similar reason (their pK_a values are approximately 6[71]). The Thr-199 residue may also carry a positive charge during part of the reaction cycle to aid deprotonation of H_2O and removal of bicarbonate from the first shell.[21] We conclude that the enzyme may be able to disperse the positive charge around the Zn^{2+} center and its immediate surroundings to the neighboring groups in order to promote an effective nucleophilic attack by the coordinated OH^- group.

Acknowledgment. The authors gratefully acknowledge financial support from the Deutsche Forschungsgemeinschaft, Fonds der Chemischen Industrie, and the Volkswagen-Stiftung. We thank Professor R. Rowlett for initial discussions on carbonic anhydrase catalysis.

Supporting Information Available: Initial rate of CO_2 hydration, $v^h_{initial}$ versus buffer concentration [B], in the $[CO_2]$ independent region (supplementary Figure 1a); plot of $[E]/v^h_{initial}$ versus 1/[B] for the data in supplementary Figure 1a (supplementary Figure 1b); initial rate of CO_2 hydration, $v^h_{initial}$ versus buffer concentration [B], in the $[CO_2]$ dependent region (supplementary Figure 2a); plot of $[E]/v^h_{initial}$ versus 1/[B] for the data in supplementary Figure 2a (supplementary Figure 2b); initial rate of CO_2 hydration versus $[CO_2]$ in the [B]-independent region (supplementary Figure 3a); plot of $1/v^h_{initial}$ versus $1/[CO_2]$ for the data in supplementary Figure 3a (supplementary Figure 3b); dependence of $\ln(k^h_{cat})$ versus pressure in both [B]-dependent and [B]-independent regions (supplementary Figure 4); plot of $\ln(k^h_{cat}/K^h_m)$ versus pressure in the [B]-dependent region (supplementary Figure 5). Initial rate of HCO_3^- hydration versus buffer concentration in the $[HCO_3^-]$ dependent region (supplementary Figure 6); Initial rate of HCO_3^- hydration versus buffer concentration in the $[HCO_3^-]$-dependent region (supplementary Figure 7); initial rate of HCO_3^- hydration versus $[HCO_3^-]_0$ in the $[HB^+]$-independent region (supplementary Figure 8a); plot of $1/v^d_{initial}$ versus $1/[HCO_3^-]_0$ for the data in supplementary Figure 8a (supplementary Figure 8b). Kinetic parameters for the hydration reaction: intermolecular proton transfer k_5, buffer concentration, $[B]_c$, at which the rate-determining step changes, turnover number (k^h_{cat}), catalytic rate constant (k^h_{cat}/K^h_m) and Michaelis−Menten constant (K^h_m) (supplementary Table I); rate constants,

k^h_{cat} ($\times 10^{-5}$ s^{-1}), at different pressures and buffer concentrations (supplementary Table II); values of k^h_{cat}/K^h_m at different pressures and buffer concentrations (supplementary Table III); dehydration rate constants, k^d_{cat}, k^h_{cat}/K^h_m, and k^d, at different pressures, and in both H_2O and D_2O solutions (supplementary Table IV) (19 pages). Ordering information is given on any current masthead page.

References and Notes

(1) (a) van Eldik, R. *Inorganic High Pressure Chemistry: Kinetics and Mechanisms*; Elsevier: Amsterdam, 1986; Chapter 1. (b) van Eldik, R.; Asano, T.; Le Noble, W. *J. Chem. Rev.* **1989**, *89*, 549.

(2) van Eldik, R.; Merbach, A. E. *Comments Inorg. Chem.* **1992**, *12*, 341.

(3) van Eldik, R. In *Perspectives in Coordination Chemistry*; Williams A. F., Floriani C., Merbach, A. E., Eds.; VHCH: Basel, 1992; p 55.

(4) van Eldik, R. In *High Pressure Chemistry, Biochemistry and Materials Science*; Winter, R., Jonas, J., Eds.; Kluwer: Dordrecht, 1993; pp C401, 329.

(5) (a) Morild, E. *Adv. Protein Chem.* **1981**, *34*, 93. (b) Butz, P.; Greulich, K. O.; Ludwig, H. *Biochemistry* **1988**, *27*, 1556. We are indebted to a referee for specifying these references for us.

(6) Prince, R. H.; Woolley, P. R. *J. Chem. Soc., Dalton Trans.* **1972**, 1548.

(7) Williams, T. J.; Henkens, R. W. *Biochemistry* **1985**, *24*, 2459.

(8) Sen, A. C.; Tu, C. K.; Thomas, H.; Wynns, G. C.; Silverman, D. N. In *Zinc Enzymes*; Bertini, I.; Luchinat, C., Maret, W., Zeppezauer, M., Eds.; Birkhäuser: Boston, 1986; Vol. I, p 329.

(9) Bauer, C.; Gros, G.; Bartels, H. *Biophysics and Physiology of Carbon Dioxide*; Springer-Verlag: New York, 1980.

(10) Woolley, P. *Nature* **1975**, *258*, 677.

(11) Bertini, I.; Luchinat, C. *Acc. Chem. Res.* **1983**, *16*, 272.

(12) Pocker, Y.; Deits, T. L. *J. Am. Chem. Soc.* **1982**, *104*, 2424.

(13) Steiner, H.; Jonsson, B.-H.; Lindskog, S. *Eur. J. Biochem.* **1975**, *59*, 253.

(14) Silverman, D. N.; Tu, C. K. *J. Am. Chem. Soc.* **1975**, *97*, 2263.

(15) Simonsson, I.; Jonsson, B.-H.; Lindskog, S. *Eur. J. Biochem.* **1979**, *93*, 409.

(16) Kogut, K. A.; Rowlett, R. S. *J. Biol. Chem.* **1987**, *262*, 16417.

(17) Botre, F.; Gros, G.; Storey, B. T. *Carbonic Anhydrase*; VCH, Verlagsgesellschaft: D-6940, Weinheim, Germany, 1991.

(18) Merz, Jr., K. M.; Hoffmann, R.; Dewar, M. J. S. *J. Am. Chem. Soc.* **1989**, *111*, 5636.

(19) Merz, Jr., K. M. *J. Am. Chem. Soc.* **1990**, *112*, 7973.

(20) Jacob, O.; Cardenas, R.; Tapia, O. *J. Am. Chem. Soc.* **1990**, *112*, 8692.

(21) Krauss, M.; Garmer, D. R. *J. Am. Chem. Soc.* **1991**, *113*, 6426.

(22) Merz, Jr., K. M. *J. Am. Chem. Soc.* **1991**, *113*, 406.

(23) Aqvist, J.; Fothergill, M.; Warshel, A. *J. Am. Chem. Soc.* **1993**, *115*, 631.

(24) Kitajima, N.; Hikichi, S; Tanaka, M; Moro-oka, Y. *J. Am. Chem. Soc.* **1993**, *115*, 5496.

(25) Peng, Z.; Merz, Jr., K. M. *J. Am. Chem. Soc.* **1993**, *115*, 9640.

(26) Warshel, A.; Sussman, F.; Hwang, K. *J. Mol. Biol.* **1988**, *201*, 139.

(27) Sola, M.; Lledos, A.; Duran, M.; Bertran, J. *J. Am. Chem. Soc.* **1992**, *114*, 869.

(28) Garmer, D. R.; Krauss, M. *J. Am. Chem. Soc.* **1992**, *114*, 6847.

(29) Bertini, I.; Mangani, S.; Pierattelli, R. *International Conference on Carbon Dioxide Utilization*; Sept. 1993, lectures and posters, Bari, Italy; p 223.

(30) Behravan, G.; Jonsson, B.-H.; Lindskog, S. *Eur. J. Biochem* **1990**, *190*, 351.

(31) Silverman, D. N.; Lindskog, S. *Acc. Chem. Res.* **1988**, *21*, 30.

(32) Kannan, K. K.; Petef, M.; Fridborg, K.; Lövgren, S.; Ohlsson, A. *Proc. Natl. Acad. Sci. U.S.A.* **1975**, *72*, 51.

(33) Kannan, K. K.; Petef, M.; Fridborg, K.; Cid-Dresdner, H.; Lövgren, S. *FEBS Lett.* **1977**, *73*, 115.

(34) Liljas, A.; Kannan, K. K.; Bergsten, P.-C.; Warra, I.; Fridborg, K.; Strandberg, B.; Carlbom, U.; Järup, L; Lövgren, S.; Petef, M. *Nature New Biol.* **1972**, *235*, 131.

(35) Eriksson, E. A.; Jones, T. A.; Liljas, A. In *Zinc Enzymes*; Bertini, I., Luchinat, C., Maret, W., Zeppezauer, M., Eds.; Birkhäuser: Boston, 1986; Vol. I, p 317.

(36) Nair, S. K.; Calderone, T. L.; Christianso, D. W.; Fierke, C. A. *J. Biol. Chem.* **1991**, *266*, 17320.

(37) Fierke, C. A; Calderone, T. L.; Krebs, J. F. *Biochemistry* **1991**, *30*, 11054.

(38) Bertini, I.; Canti, G.; Luchinat, C.; Borghi, E. *J. Inorg. Biochem.* **1983**, *18*, 221.

(39) Bertini, I.; Luchinat, C.; Monnanni, R.; Rodens, S.; Moratal Mascarell, J. M. *J. Am. Chem. Soc.* **1987**, *109*, 7855.

(40) Pocker, Y.; Janjic, N. *J. Am Chem. Soc.* **1989**, *111*, 731.

(41) Ghannam, A. F.; Tsen, W.; Rowlett, R. S. *J. Biol. Chem.* **1986**, *261*, 1164.

(42) Rowlett, R. S. *J. Protein Chem.* **1984**, *3*, 369.

(43) Lindskog, S. *J. Mol. Catal.* **1984**, *23*, 357.

(44) (a) Lindskog, S. In *Zinc Enzymes*; Spiro, T. G., Ed.; Wiley: New York, 1983; p 77. (b) Pullman, A. *Ann. N.Y. Acad. Sci.* **1981**, *367*, 340 and references therein.

(45) Looney, A.; Han, R.; McNeill, K.; Parkin, G. *J. Am. Chem. Soc.* **1993**, *115*, 4690.

(46) Spitzer, U.; van Eldik, R.; Kelm, H. *Inorg. Chem.* **1982**, *21*, 2821.

(47) Mozhaev, V. V.; Heremans, K.; Frank, J.; Masson, P.; Balny, C. *Tibtech* **1994**, *12*, 493.

(48) van Eldik, R.; Palmer, D. A. *J. Solut. Chem.* **1982**, *11*, 339.

(49) Coleman, J. E. *J. Biol. Chem.* **1967**, *242*, 5212.

(50) Kahlifah, R. G. *J. Biol. Chem.* **1971**, *246*, 2561.

(51) Pocker, Y.; Bjorquist, D. W. *Biochemistry* **1977**, *16*, 5698.

(52) van Eldik, R.; Palmer, D. A.; Schmidt, R.; Kelm, H. *Inorg. Chim. Acta* **1981**, *50*, 131.

(53) Rowlett, R. S.; Silverman, D. N. *J. Am. Chem. Soc.* **1982**, *104*, 6737.

(54) de Levie, R. *J. Chem. Educ.* **1986**, *63*, 10.

(55) Gibbons, B. H.; Edsall, J. T. *J. Biol. Chem.* **1963**, *238*, 3504.

(56) Zhang, X.; van Eldik, R.; Koike, T.; Kimura, E. *Inorg. Chem.* **1993**, *32*, 5749.

(57) Kitamura, Y.; Itoh, T. *J. Solut. Chem.* **1987**, *16*, 715.

(58) King, E. L.; Altman, G. *J. Phys. Chem.* **1956**, *60*, 1376.

(59) Millero, F. J.; Laferriere, A. L.; Chetirkin, P. V. *J. Phys. Chem.* **1977**, *81*, 1737.

(60) Keister, J. B.; Frey, U.; Zbinden, D.; Merbach, A. E. *Organometallics* **1991**, *10*, 1497.

(61) Swaddle, T. W. *Inorg. Chem.* **1980**, *19*, 3203.

(62) Ohtako, H.; Yamatera, H. *Structure and Dynamics of Solutions*; Elsevier: Amsterdam, 1992; p 264.

(63) Lipscomb, W. N. *Annu. Rev. Biochem.* **1983**, *52*, 17.

(64) Sola, M.; Liedos, A.; Duran, M.; Bertran J. *J. Am. Chem. Soc.* **1992**, *114*, 869 and references therein.

(65) Eriksen, J.; Mønsted, L.; Mønsted O. *Acta Chem. Scand.* **1992**, *46*, 52.

(66) Lesburg, C. A.; Christianson, D. W. *J. Am. Chem. Soc.* **1995**, *117*, 6838.

(67) Lindskog, S. In: Bertini, L., Luchinat, C., Maret, W., Zeppezauer, M., Eds.; *Zinc Enzymes*; Birkhäuser: Boston, MA, 1986; Chapter 22, p 307.

(68) Yachandra, V.; Powers, L.; Spiro, T. G. *J. Am. Chem. Soc.* **1983**, *105*, 6596.

(69) Zhang, X.; van Eldik, R. *Inorg. Chem.* **1995**, *34*, 5606.

(70) Hay, R. W. *Bio-Inorganic Chemistry*; Ellis Horwood: Chichester, England, 1984; p 29.

(71) Bertini, I.; Luchinat, C.; Scozzatava A. *Inorg. Chim. Acta* **1980**, *46*, 85.

JP9524791